

Cite this: DOI: 10.1039/d1ew00446h

## Labile carbon release from oxic–anoxic cycling in woodchip bioreactors enhances nitrate removal without increasing nitrous oxide accumulation†

Philip M. McGuire, <sup>a</sup> Valentina Dai, <sup>a</sup> M. Todd Walter<sup>b</sup> and Matthew C. Reid <sup>\*a</sup>

Denitrification in woodchip bioreactors (WBRs) treating agricultural drainage and runoff is frequently carbon-limited due to the recalcitrance of carbon (C) in lignocellulosic woodchip biomass. Recent research has shown that redox fluctuations, achieved through periodic draining and re-flooding of WBRs, can increase nitrate removal rates by enhancing the release of labile C during oxic periods. While drying–rewetting (DRW) cycles appear to hold great promise for improving the performance of denitrifying WBRs, redox fluctuations in nitrogen-rich environments are commonly associated with enhanced emissions of the greenhouse gas nitrous oxide ( $N_2O$ ) due to inhibition of  $N_2O$  reduction in microaerophilic conditions. Here, we evaluate the effects of oxic–anoxic cycling associated with DRW on the quantity and quality of C mobilized from woodchips, nitrate removal rates, and  $N_2O$  accumulation in a complementary set of flow-through and batch laboratory bioreactors at 20 °C. Redox fluctuations significantly increased nitrate removal rates from 4.8–7.2 g N m<sup>−3</sup> d<sup>−1</sup> in a continuously saturated (CS) reactor to 9.8–11.2 g N m<sup>−3</sup> d<sup>−1</sup> 24 h after a reactor is drained and re-saturated. Results support the theory that DRW conditions lead to faster  $NO_3^-$  removal rates by increasing mobilization of labile organic C from woodchips, with lower aromaticity in the dissolved C pool of oxic–anoxic reactors highlighting the importance of lignin breakdown to overall carbon release. There was no evidence for greater  $N_2O$  accumulation, measured as  $N_2O$  product yields, in the DRW reactors compared to continuously saturated reactors. We propose that greater organic C availability for  $N_2O$  reducers following oxic periods outweighs the effect of microaerophilic inhibition of  $N_2O$  reduction in controlling  $N_2O$  dynamics. Implications of these findings for optimizing DRW cycling to enhance nitrate removal rates in denitrifying WBRs are discussed.

Received 29th June 2021,  
Accepted 4th October 2021

DOI: 10.1039/d1ew00446h

rsc.li/es-water

### Water impact

Oxic–anoxic cycling has been identified as a practical method to overcome carbon-limited conditions in denitrifying woodchip bioreactors treating agricultural tile drainage, but the effects of these water management practices on production of the greenhouse gas nitrous oxide ( $N_2O$ ) have not been evaluated. Here, we use laboratory-scale bioreactors to show that oxic–anoxic cycling significantly enhances nitrate removal rates without systematically increasing  $N_2O$  production, even during the transition from oxic to anoxic conditions. Our findings provide new insights into how oxic–anoxic cycling boosts nitrogen metabolism by changing the quantity and quality of organic carbon mobilized from woodchips.

## 1. Introduction

Woodchip bioreactors (WBRs) are growing in popularity as a sustainable technology for nitrate ( $NO_3^-$ ) removal from nonpoint sources including agricultural tile drainage,<sup>1</sup> stormwater runoff,<sup>2</sup> and wastewater effluent.<sup>3</sup> WBRs use lignocellulosic woodchips as a slow-release carbon (C) source

and biofilm support structure, and are designed to enhance heterotrophic denitrification at terrestrial-aquatic interfaces and thereby decrease  $NO_3^-$  loads to aquatic environments. An estimated 50% of reactive nitrogen (N) derived from anthropogenic land-based activities is transported to coastal waters,<sup>4</sup> and there is great interest in the potential of WBRs to control  $NO_3^-$  loads to N-limited coastal systems. However, there are concerns regarding the long-term effectiveness of WBRs as the pool of labile woodchip-derived C is depleted.<sup>5–8</sup>

Denitrification in  $NO_3^-$  rich environments, including WBRs as well as wetlands and riparian zones, is frequently C-limited.<sup>5,7,9–12</sup> In WBRs this is due to the recalcitrance of C in lignin-rich woody biomass,<sup>13</sup> particularly in flooded anaerobic

<sup>a</sup> School of Civil and Environmental Engineering, Cornell University, Ithaca, NY 14853, USA. E-mail: mcr239@cornell.edu

<sup>b</sup> Department of Biological and Environmental Engineering, Cornell University, Ithaca, NY 14853, USA

† Electronic supplementary information (ESI) available. See DOI: 10.1039/d1ew00446h

conditions where oxidative decomposition processes are inhibited. Readily-hydrolyzed fractions of woodchip C are typically leached from WBRs during the first one to two years of operation, with effluent characterized by dissolved organic carbon (DOC) concentrations of 20–80 mg C/L during this period.<sup>8,14</sup> As woodchips age, however, DOC concentrations decrease significantly due to protective lignin sheaths that hinder access to more readily bioavailable cellulosic and hemicellulosic C sources.<sup>15</sup> DOC in a WBR effluent decreased from 20.7 mg C/L to 3.0 mg C/L over the first 240 days of operation<sup>8</sup> and WBRs older than 2 years are typically characterized by DOC concentrations between 1–4 mg C/L.<sup>16,17</sup> This decrease in soluble carbon is observed in conjunction with slower denitrification rates.<sup>18</sup> In addition to diminished  $\text{NO}_3^-$  removal rates, C-limited conditions in denitrifying environments can also be associated with greater accumulation of nitrous oxide ( $\text{N}_2\text{O}$ ),<sup>19,20</sup> an important greenhouse gas and ozone-depleting substance.<sup>21</sup> Efforts to overcome C-limitation in WBRs have included supplemental dosing with exogenous labile C<sup>22–24</sup> but this can be difficult to operationalize in practice in decentralized WBR systems.

Recent research with woodchip media from a 6-year old WBR has demonstrated that periodic redox fluctuations, achieved by drying and rewetting the reactor, increase nitrate removal rates as well as concentrations of total C and DOC concentration in WBR effluent.<sup>25,26</sup> The authors linked the faster  $\text{NO}_3^-$  removal to greater C bioavailability, presumably driven by enhanced decomposition of woodchip biomass during oxic periods.<sup>25,27</sup> However, other studies did not observe increased  $\text{NO}_3^-$  removal rates following drying-rewetting of WBRs.<sup>28</sup> While drying-rewetting (DRW) cycles may be beneficial for accelerating denitrification rates in some cases, they are typically associated with enhanced  $\text{N}_2\text{O}$  emissions,<sup>29</sup> as the  $\text{N}_2\text{O}$  reductase enzyme, NosZ, is more sensitive to oxygen ( $\text{O}_2$ ) inhibition than upstream N-reducing enzymes that reduce  $\text{NO}_3^-$  to  $\text{N}_2\text{O}$ .<sup>30–33</sup> This can lead to  $\text{N}_2\text{O}$  accumulation in microaerophilic environments, and oxic-anoxic cycling in soils often increases  $\text{N}_2\text{O}$  production and emissions.<sup>34,35</sup> A recent study with a WBR experiencing DRW cycles showed an increase in dissolved  $\text{N}_2\text{O}$  concentrations one day after re-saturation.<sup>28</sup>

The objective of this study was to clarify the impact of redox fluctuations on coupled N and C metabolisms in WBRs, with a focus on N dynamics in the oxic-anoxic transition following the re-saturation of woodchip media. We originally hypothesized that DRW cycles would increase  $\text{NO}_3^-$  removal rates by increasing bioavailable C but would simultaneously increase the undesirable production and export of  $\text{N}_2\text{O}$  from WBRs.

## 2. Materials and methods

### Model woodchip bioreactor flowthrough experiments

Horizontally oriented laboratory model woodchip bioreactors (1.5 m length  $\times$  0.1 m inner diameter) were constructed in duplicate using PVC pipe with 8 ports for sampling of

solutes, including dissolved gases, installed along the length of the reactors (Fig. S1 and S2†). Dissolved oxygen (DO) was measured *via* needle-type oxygen microsensors (Presens, Germany) inserted through septa at 55 cm (“upstream”) and 105 cm (“downstream”). Reactor media consisted of Ash (*Fraxinus* sp.) woodchips collected from a 7-year-old bioreactor treating agricultural tile drainage at the Homer C. Thompson Vegetable Farm in Freeville, New York, USA.<sup>36</sup> The field bioreactor is continuously saturated, with the exception of infrequent, extended dry periods when water levels inside the bioreactor can fall somewhat. Woodchips were rectangular in shape and averaged approximately 4 cm length  $\times$  2 cm width  $\times$  0.5 cm thickness. Woodchips were packed by hand into the reactors with periodic shaking to allow woodchips to settle and to facilitate a uniform porosity within and between reactors. Woodchips were maintained in the reactors under fully saturated, continuous flow conditions for 2 months prior to the beginning of the experiments described here. The drainable porosity, equivalent to the effective porosity,<sup>37</sup> was determined as the volume of water drained from the woodchip media divided by the woodchip-filled volume of the reactor. The specific retention<sup>17</sup> was determined as the difference in mass between wet and dry woodchips after drying overnight at 105 °C. Both drainable porosity and specific retention were measured from a homogenous mixture from both reactors following the conditioning period but prior to starting the experiment. Total porosity was calculated as the sum of drainable porosity and specific retention. Reactor influent containing 40 mg L<sup>-1</sup>  $\text{NO}_3^-$  as  $\text{NaNO}_3$ , 2.5 mg L<sup>-1</sup>  $\text{NH}_4^+$  as  $\text{NH}_4\text{Cl}$ , and 1.8 mg L<sup>-1</sup>  $\text{PO}_4^{3-}$  as  $\text{Na}_2\text{HPO}_4$  at an average pH of 7.7 was fed into the reactors to achieve an approximate hydraulic retention time (HRT) of 12 hours. The influent was not degassed prior to being pumped into the reactor.

5- and 8-week experiments (experiments 1 and 2, respectively, Table 1) were performed to evaluate the impacts of redox fluctuations on  $\text{NO}_3^-$  removal rates,  $\text{N}_2\text{O}$  production, and C transformations in each reactor. Experiments were conducted at approximately 20 °C, similar to other laboratory bioreactor experiments<sup>16,17</sup> and to temperatures recorded in Central New York bioreactors in late summer  $\sim$ 18 °C (data not shown). Each experiment included a continuously saturated (CS) and DRW reactor. Between experiments, woodchips were removed from reactors, homogenized, and redistributed to both reactors to ensure similar starting media. The DRW reactor was subject to weekly drying-rewetting cycles, with 5 days of saturation followed by a 48 h dry period before being reflooded (Fig. S3†). Reactor drainage took approximately 2 hours. The CS reactor was operated under saturated flow conditions for the duration of the experiments. As woodchips in experiment 1 and experiment 2 experienced different antecedent conditions (e.g., approximately half of the woodchips in the continuously-saturated bioreactor in experiment 2 would have experienced DRW conditions during experiment 1), these experiments should not be considered replicates of one another. However,

Table 1 Experimental designs and descriptions

Reactor design	Replicates and duration	Experiment name and abbreviation	Description
Flowthrough	Two replicates, each with a continuously saturated and a drying–rewetting reactor. The first replicate lasted 5 weeks and the second replicate lasted 8 weeks. There was one drying–rewetting cycle per week in the DRW reactor	Continuously saturated (CS) Drying–rewetting (DRW)	Reactors were kept under saturated flow conditions for the duration of the experiment
Batch	Triplicate sets of both anoxic and oxic–anoxic reactors operated for 2 weeks	Anoxic reactor (AR) Oxic–anoxic reactor (OAR)	Reactors were subjected to weekly draining-reflooding cycles, with 5 days of saturation followed by a 48 hour dry period before being reflooded Maintained under permanently anoxic conditions

as they are long-term experiments, weekly samplings can be interpreted as replicates of one another.

Bromide ( $\text{Br}^-$ ) tracer tests were used to estimate pore velocity and dispersion *via* fits to a 1-dimensional advection-dispersion equation:

$$\frac{\partial C}{\partial t} = D \frac{\partial^2 C}{\partial x^2} - v \frac{\partial C}{\partial x} \quad (1)$$

where  $c$  is the  $\text{Br}^-$  concentration [ $\text{M L}^{-3}$ ],  $D$  is the dispersion coefficient [ $\text{L}^2 \text{T}^{-1}$ ], and  $v$  is the pore-water velocity [ $\text{L T}^{-1}$ ].  $\text{Br}^-$  breakthrough curves were fit using the CXTFIT package of STANMOD<sup>38,39</sup> to estimate  $v$  and  $D$ . The mean residence time (MRT) associated with each sampling port at a distance  $L$  along a reactor was calculated as  $L/v$ .

### Sample collection and analysis

Routine sampling was conducted twice per week, corresponding to 1 day and 4 days after re-flooding of the DRW reactor and collected from ports along the length of the reactor (Fig. S1†). Water samples were immediately filtered through a 0.22-micron membrane filter prior to analysis *via* ion chromatography (Thermo Scientific Dionex ICS-2100) and dissolved organic carbon (DOC) using the non-purgeable organic carbon (NPOC) method (Shimadzu TOC-L). Samples were analyzed within one week of collection. Samples for dissolved gas analysis were also collected from reactor ports and were not filtered but preserved in 50 mM sodium azide in 9 mL crimp-sealed vials. A nitrogen ( $\text{N}_2$ ) headspace of approximately 5 mL (actual volume was verified gravimetrically) was introduced, equilibrated with the water by shaking the vial for at least 5 minutes, and analyzed with a gas chromatograph (GC) equipped with an electron capture detector for  $\text{N}_2\text{O}$  and a flame ionization detector for methane ( $\text{CH}_4$ ), with a methanizer for analysis of carbon dioxide ( $\text{CO}_2$ ) (Shimadzu GC-2014). Vials were held at room temperature for no longer than 2 hours prior to  $\text{N}_2$  introduction and analyzed within 12 hours of equilibration. In experiment 2, pH was measured in all samples using a portable pH electrode (Thermo Orion) immediately after samples were collected from the reactor. High frequency sampling, which is

characterized by sample collection every few hours immediately following rewetting, was performed during experiment 2 to examine changes in DO, N species, and carbon during the transition from oxic to anoxic conditions, and the potential for biogeochemical “hot moments” of  $\text{N}_2\text{O}$  production due to microaerophilic conditions.<sup>40,41</sup> In high frequency sampling, only the central four reactor ports (from 36 cm to 125 cm) were sampled for each timepoint.

$\text{NO}_3^-$  removal rates were determined as the slope of a least-squares linear model fit to longitudinal  $\text{NO}_3^-$  concentration profiles as a function of MRT and then multiplied by the effective porosity of the reactor to report removal rates normalized by total reactor volume. This zero-order modeling of  $\text{NO}_3^-$  removal rates appropriately describes  $\text{NO}_3^-$  removal rates under the range of  $\text{NO}_3^-$  concentrations used here,<sup>16,17</sup> though a recent study has questioned the use of zero-order kinetics with influent  $\text{NO}_3^-$  concentrations  $< 10 \text{ mg NO}_3^- \text{ N/L}$ .<sup>12</sup>  $\text{NO}_3^-$  removal efficiency was calculated as:

$$\text{NO}_3^- \text{ Removal Efficiency} = \frac{\text{NO}_{3,i}^- - \text{NO}_{3,e}^-}{\text{NO}_{3,i}^-} \times 100 \quad (2)$$

$\text{N}_2\text{O}$  production was evaluated as an “effective  $\text{N}_2\text{O}$  yield”, with  $\text{N}_2\text{O}$  production along a length of the reactor normalized by the removal of  $\text{NO}_3^-$  along that length:

$$\text{N}_2\text{O Yield} = \frac{\text{N}_2\text{O}_i - \text{N}_2\text{O}_0}{-(\text{NO}_{3,i}^- - \text{NO}_{3,0}^-)} \quad (3)$$

where  $\text{N}_2\text{O}_i$  is the  $\text{N}_2\text{O}$ -N concentration at a downstream port  $i$  [ $\text{M L}^{-3}$ ],  $\text{N}_2\text{O}_0$  is the  $\text{N}_2\text{O}$ -N concentration in the reactor inlet [ $\text{M L}^{-3}$ ],  $\text{NO}_{3,i}^-$  is the  $\text{NO}_3^-$ -N concentration at a downstream port  $i$  [ $\text{M L}^{-3}$ ], and  $\text{NO}_{3,0}^-$  is the  $\text{NO}_3^-$ -N concentration in the reactor inlet [ $\text{M L}^{-3}$ ]. For high frequency sampling,  $i$  represents the sampling port at 125 cm, while  $o$  represents the sampling port at 36 cm.

Dissolved inorganic carbon (DIC) was determined using headspace GC measurements of  $\text{CO}_2$  partial pressure in conjunction with pH and carbonate equilibrium models.<sup>42</sup> We assumed that ionic strength effects were negligible.

## Woodchip bioreactor batch experiments

Woodchip batch experiments in 250 mL media bottles were performed with the objective of characterizing effects of antecedent oxic periods on the quantity and quality of organic C mobilized from lignocellulosic woodchips. Media bottles were closed with bromobutyl rubber stoppers to allow liquid to be extracted from anoxic reactors. Ash woodchips, collected from the bioreactor at the Homer C. Thompson Vegetable Farm, were initially incubated in a synthetic media solution of 200 mg L<sup>-1</sup> NO<sub>3</sub><sup>-</sup> as NaNO<sub>3</sub>, 250 mg L<sup>-1</sup> KCl, 84 mg L<sup>-1</sup> NaHCO<sub>3</sub>, 24 mg L<sup>-1</sup> NaH<sub>2</sub>PO<sub>4</sub>, and a trace element solution (Table S1†) for approximately 72 hours in anoxic conditions. 110 g of wet weight woodchips per reactor were then separated into two sets of triplicate batch reactors maintained in the dark. Anoxic reactors were kept permanently anoxic, while oxic-anoxic reactors were aerated for 24 h *via* air sparging, sealed anoxically for 24 h, aerated for 96 h, sealed anoxically for 48 h, and then aerated for 6 days. Following these conditioning steps, both anoxic and oxic-anoxic reactors were decanted, rinsed with the batch reactor synthetic media solution, and then refilled with the batch reactor synthetic media solution. All reactors were sparged with N<sub>2</sub> for 1 hour and then incubated anoxically in the dark with gentle shaking. Samples collected over the next ~120 hours were filtered and analyzed for DOC and for NO<sub>3</sub><sup>-</sup> and low molecular weight organic acids *via* ion chromatography. Samples were collected approximately every 1–2 h for the first 10 h and then sampling was relaxed to 1–2 samples per day for the final ~100 h. Aromaticity of the soluble C pool was assessed *via* specific ultraviolet absorbance (SUVA<sub>254</sub>).<sup>43</sup> Absorbance at 254 nm was determined using a UV-vis spectrophotometer (Shimadzu UV-2600) and was normalized by the DOC concentration.

## Statistical methods

Statistically significant differences among means under different hydraulic regimes were evaluated *via* one-way ANOVA, Welch one-way ANOVA, or Kruskal–Wallis rank sum tests as appropriate (Table 2). ANOVA assumptions of homogeneity of variance and normality were assessed *via* Levene's test and Shapiro–Wilk test, respectively. Multiple pairwise-comparisons were evaluated using either Tukey's honest significant difference, Games–Howell, or Wilcoxon rank sum *post hoc* tests. Statistical analyses were implemented in R<sup>44</sup> and evaluated at the 95% confidence level.

**Table 2** Statistical tool summary

Examined metric	Experiment replicate	ANOVA assumption validity		Resulting statistical analysis tool	<i>Post-hoc</i> test
		Homogeneity of variance	Normality		
Exported nitrate	1	✗	✗	Kruskal–Wallis rank sum	Wilcoxon rank sum
	2	✗	✓	Welch one-way ANOVA	Games–Howell
Nitrate removal rate	1	✓	✓	ANOVA	Tukey
	2	✓	✓	ANOVA	Tukey
N <sub>2</sub> O yield	1	✓	✓	ANOVA	Tukey
	2	✗	✓	Welch one-way ANOVA	N/A: no difference among means

## 3. Results

### Bioreactor hydrodynamics and redox cycling

The effective porosity and specific retention were determined to be 0.58 and 0.31, respectively – similar to previously reported values for woodchip media.<sup>45</sup> Total porosity was 0.89. Mean hydraulic retention times (MRTs) determined from bromide tracer tests were similar to each other, ranging from 13.4 to 16.0 hours (Table 3, Fig. S4–S7†). Additional hydraulic parameters are reported in the ESI† (Table S2). DO concentrations were commonly <0.1 mg L<sup>-1</sup> in the CS reactor (Fig. S8–S11†). In the DRW reactor, O<sub>2</sub> levels immediately increased when reactors were drained and the reactor volume filled with atmospheric air. O<sub>2</sub> levels then slowly decreased over the 48 hour dry period before declining quickly (<2 h) to <0.3 mg L<sup>-1</sup> when reactors were re-saturated and the DO sensors re-submerged (Fig. 1 and S12–S14†). We acknowledge that the downstream DO sensor in the CS reactor records higher DO concentrations than the upstream sensor, an unexpected result (Fig. S9 and S11†). This was attributed to a leak in the septum where the “needle-type” microsensor pierces a septum to enter the reactor, so we expect this to be a localized phenomenon that would not impact a large fraction of the reactor.

### Nitrogen transformations

DRW reactors exhibited greater overall mean ± s.d. NO<sub>3</sub><sup>-</sup> removal efficiencies, (90.1 ± 11.9 and 94.1 ± 7.8% removal in experiments 1 and 2, respectively) than CS reactors (46.7 ± 4.2 and 72.9 ± 12.9% removal) (Fig. 2A and B) and faster NO<sub>3</sub><sup>-</sup> removal rates (Fig. 2C and D). In experiment 1, mean exported NO<sub>3</sub><sup>-</sup> concentrations were 20.20 ± 4.59, 1.09 ± 0.28, and 5.05 ± 3.62 mg L<sup>-1</sup> NO<sub>3</sub><sup>-</sup> in CS, DRW 1-day post re-saturation (DRW-1), and DRW 4 days post re-saturation (DRW-4), respectively. Statistically significant differences were observed between CS and DRW-1 (*p* = 0.002) and CS and DRW-4 (*p* = 0.002). Mean exported NO<sub>3</sub><sup>-</sup> concentrations between DRW-1 and DRW-4 were not significantly different (*p* = 0.151). In experiment 2, mean exported NO<sub>3</sub><sup>-</sup> concentrations were 12.2 ± 5.70, 0.43 ± 0.40, and 4.79 ± 3.87 mg L<sup>-1</sup> NO<sub>3</sub><sup>-</sup> in CS, DRW-1, and DRW-4, respectively. Statistically significant differences were observed between CS and DRW-1 (*p* < 0.001), CS and DRW-4 (*p* = 0.004), and DRW-1 and DRW-4 (*p* = 0.036).

Mean NO<sub>3</sub><sup>-</sup> removal rates are summarized in Table 3. Goodness of fit for linear models of NO<sub>3</sub><sup>-</sup> profiles from

Table 3 Nitrate removal rates and  $\text{N}_2\text{O}$  product yields

Experiment	Reactor hydraulic regime	HRT (h)	Average temperature (°C)	Average nitrate removal rate ( $\text{g N m}^{-3} \text{ day}^{-1}$ )	Average effective $\text{N}_2\text{O}$ Yield <sup>a</sup> $\text{mg N}_2\text{O-N (mg NO}_3^-\text{N)}^{-1}$
Experiment 1	Continuously saturated (CS)	15.1	19.6	$4.8 \pm 0.7$	$8.1 \times 10^{-3} \pm 2.1 \times 10^{-3}$
	Drying-rewetting (DRW)	13.4	19.6	1 day post re-saturation (DRW-1): $11.2 \pm 0.7$ 4 days post re-saturation (DRW-4): $9.6 \pm 1.3$ $7.2 \pm 0.9$ 1 day post re-saturation (DRW-1): $9.8 \pm 0.8$ 4 days post re-saturation (DRW-4): $8.1 \pm 0.5$	1 day post re-saturation (DRW-1): $1.4 \times 10^{-4} \pm 6.4 \times 10^{-4}$ 4 days post re-saturation (DRW-4): $-3.6 \times 10^{-4} \pm 5.2 \times 10^{-4}$ $-2.7 \times 10^{-4} \pm 2.4 \times 10^{-3}$ 1 day post re-saturation (DRW-1): $4.0 \times 10^{-4} \pm 7.1 \times 10^{-4}$ 4 days post re-saturation (DRW-4): $-7.5 \times 10^{-4} \pm 2.2 \times 10^{-3}$
Experiment 2	Continuously saturated (CS)	15.2	20.2		
	Drying-rewetting (DRW)	16.0	20.2		

<sup>a</sup> Calculated using eqn (3), where  $i$  represents the sampling port at 135 cm. <sup>b</sup> Negative value represents consumption of  $\text{N}_2\text{O}$  between sampling points.

individual sampling dates was assessed as an adjusted  $R^2$  metric, which ranged between 0.77–0.99 and averaged 0.88 across all model fits. In all cases,  $\text{NO}_3^-$  removal rates were significantly higher in DRW-1 than in CS conditions. In experiment 1, statistically significant differences were observed between CS and DRW-1 ( $p < 0.001$ ) and CS and DRW-4 ( $p < 0.001$ ), with significantly higher removal rates in the DRW reactors. There was no significant difference in  $\text{NO}_3^-$  removal rates between DRW-1 and DRW-4 ( $p = 0.059$ ). In experiment 2, significantly higher removal rates were observed in DRW-1 compared to CS conditions ( $p < 0.001$ ).  $\text{NO}_3^-$  removal rates between CS and DRW-4 were not significantly different ( $p = 0.057$ ). While  $\text{NO}_3^-$  removal in DRW reactors were similar in experiments 1 and 2,  $\text{NO}_3^-$  removal rates in CS reactors increased from experiment 1 to 2. This led to smaller differences between DRW and CS reactors in experiment 2 (Fig. 2C and D).

$\text{N}_2\text{O}$  concentration profiles are shown in Fig. 3A and B, and  $\text{N}_2\text{O}$  yields are summarized in Table 3 and Fig. 3C and D. The

$\text{N}_2\text{O}$  yield reported in Table 3 is the yield at the reactor port at 135 cm because this represents the dissolved  $\text{N}_2\text{O}$  that would be released in reactor effluent, which is the dominant  $\text{N}_2\text{O}$  release pathway from WBRs.<sup>28,46</sup>  $\text{N}_2\text{O}$  yields were highly variable from week to week, varying by up to 3 orders of magnitude in the same location in the bioreactor in the same experiment. Negative  $\text{N}_2\text{O}$  yields were commonly observed, indicating that at times the reactors served as a net sink of  $\text{N}_2\text{O}$ . This was due to non-zero  $\text{N}_2\text{O}$  in the reactor influent (Fig. 3A and B). Analysis of statistically significant differences in  $\text{N}_2\text{O}$  yields was performed by pooling all 5 or 8 weeks of data into “upstream” ports (the first three sampling ports) or “downstream” ports (the final three sampling ports).  $\text{N}_2\text{O}$  yields were generally higher in the upstream sampling ports of the DRW reactor (Fig. S15 and S16<sup>†</sup>) than the downstream ports (Fig. 3C and D), indicating net production of  $\text{N}_2\text{O}$  in upstream portions of the reactor followed by net consumption in downstream portions. In experiment 1,  $\text{N}_2\text{O}$  yields in downstream ports were significantly higher in the CS reactor than in DRW-1 ( $p < 0.001$ ) and DRW-4 ( $p < 0.001$ ), leading to lower effluent  $\text{N}_2\text{O}$  concentrations in DRW conditions (Fig. 3C). There was no significant difference between mean  $\text{N}_2\text{O}$  yields in DRW-1 and DRW-4 ( $p = 0.890$ ). This indicates that, after normalizing  $\text{N}_2\text{O}$  production by the removed concentration of  $\text{NO}_3^-$ -N, there was less production of  $\text{N}_2\text{O}$  in the DRW reactor both 1 and 4 days after re-saturation. In experiment 2, there was no significant difference in the  $\text{N}_2\text{O}$  yield between the CS and DRW reactors ( $p = 0.3$ ), and similar concentrations of dissolved  $\text{N}_2\text{O}$  were released in reactor effluent (Fig. 3B). Similar to the experimental results for nitrate removal rates, there were clearer differences in  $\text{N}_2\text{O}$  production between CS and DRW reactors in experiment 1 compared to experiment 2.

### Carbon quantity and quality

In the CS reactor, DOC concentrations were  $<4.0 \text{ mg C/L}$  for all sampling ports (Fig. 4 and S17<sup>†</sup>). There was little variation in DOC as a function of length within CS reactors, or as a function of time over the five- or eight-week duration of the experiment (Fig. S17 and S18<sup>†</sup>). DIC ranged from 9.7–33 mg C/L in CS

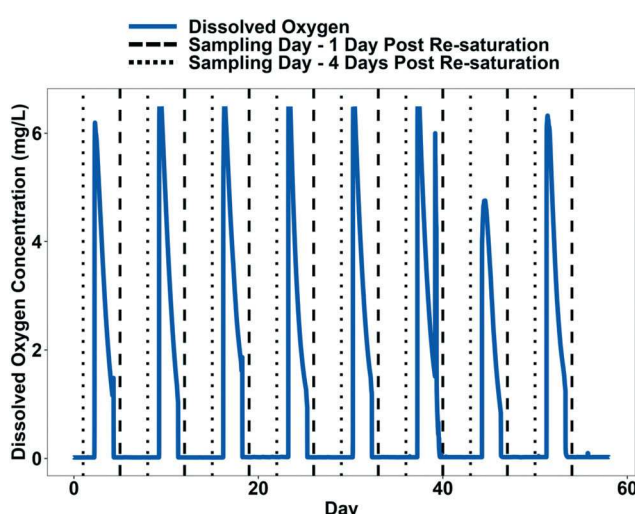
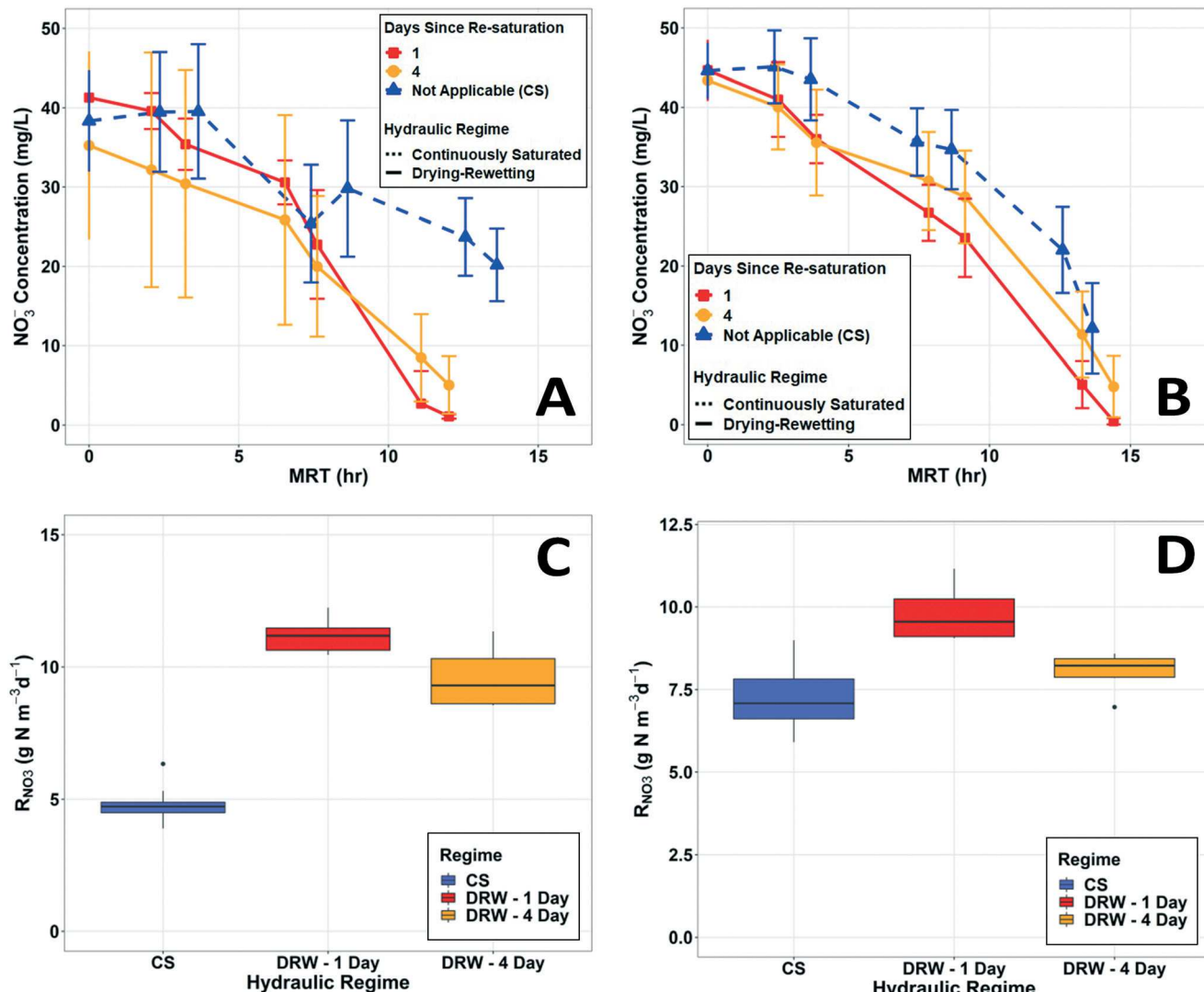


Fig. 1 Dissolved oxygen (DO) concentrations at the downstream DO sensor in the drying-rewetting bioreactor of experiment 2. The dashed and dotted lines indicate the timing of pore water sampling 1 (DRW-1) and 4 (DRW-4) days after reactor re-saturation.



**Fig. 2** (A and B) Nitrate profiles along the length of reactors. The x-axis represents distinct sampling ports, with mean residence time (MRT) determined as length along the reactor/porewater velocity. The differences in sample MRTs between CS and DRW reactors occurs because of slightly different porewater velocities. Symbols show mean values and error bars show standard deviation. (C and D) Nitrate removal rates under varying hydraulic conditions. Panels (A) and (C) are from experiment 1. Panels (B) and (D) are from experiment 2.

reactors, and were typically  $\sim 15$  mg C/L. Dissolved  $\text{CH}_4$  concentrations were negligible in the CS reactor throughout the experiment. In the DRW reactor, DOC and DIC exhibited substantial spatial and temporal variability, and in many cases were significantly higher than in the CS reactor (Fig. 4 and S19 and S20†). DOC concentrations one day post re-saturation (see example data from days 19 and 40 in Fig. 4) in the downstream half of the reactor were usually between 5–7 mg C/L, compared to 2–3 mg C/L in the CS reactor. DOC concentrations were higher in downstream sections of the DRW reactor than upstream portions. By day 4 post re-saturation, DOC concentrations for the most part had decreased to the 2–3 mg C/L range throughout the reactor. DIC concentrations, which reflect the effects of microbial respiration, ranged from 45–65 mg C/L in downstream sections of the DRW reactor on day 1 post re-saturation, decreasing to 20–30 mg C/L on day 4 post re-

saturation. Counterintuitively,  $\text{CH}_4$  concentrations were higher in the DRW reactor experiencing periodic oxic conditions than the CS reactor. In contrast to DOC and DIC,  $\text{CH}_4$  concentrations were similar on days 1 and 4 post re-saturation.

#### Transition from oxic to anoxic conditions

Results of high-frequency pore water analysis in the 20 h after reactors were re-saturated in weeks 1, 3, 6, and 8 of experiment 2 are summarized in Fig. 5. In most cases,  $\text{NO}_3^-$  removal rates across the central 89 cm of the reactor measured during high-frequency analysis were highest immediately following re-saturation and exhibited a declining trend over time. The highest observed  $\text{NO}_3^-$  removal rate ( $14.2 \text{ g NO}_3^- \text{N m}^{-3} \text{ day}^{-1}$ ) occurred during week 6 and represented an increase of 45% from the mean nitrate

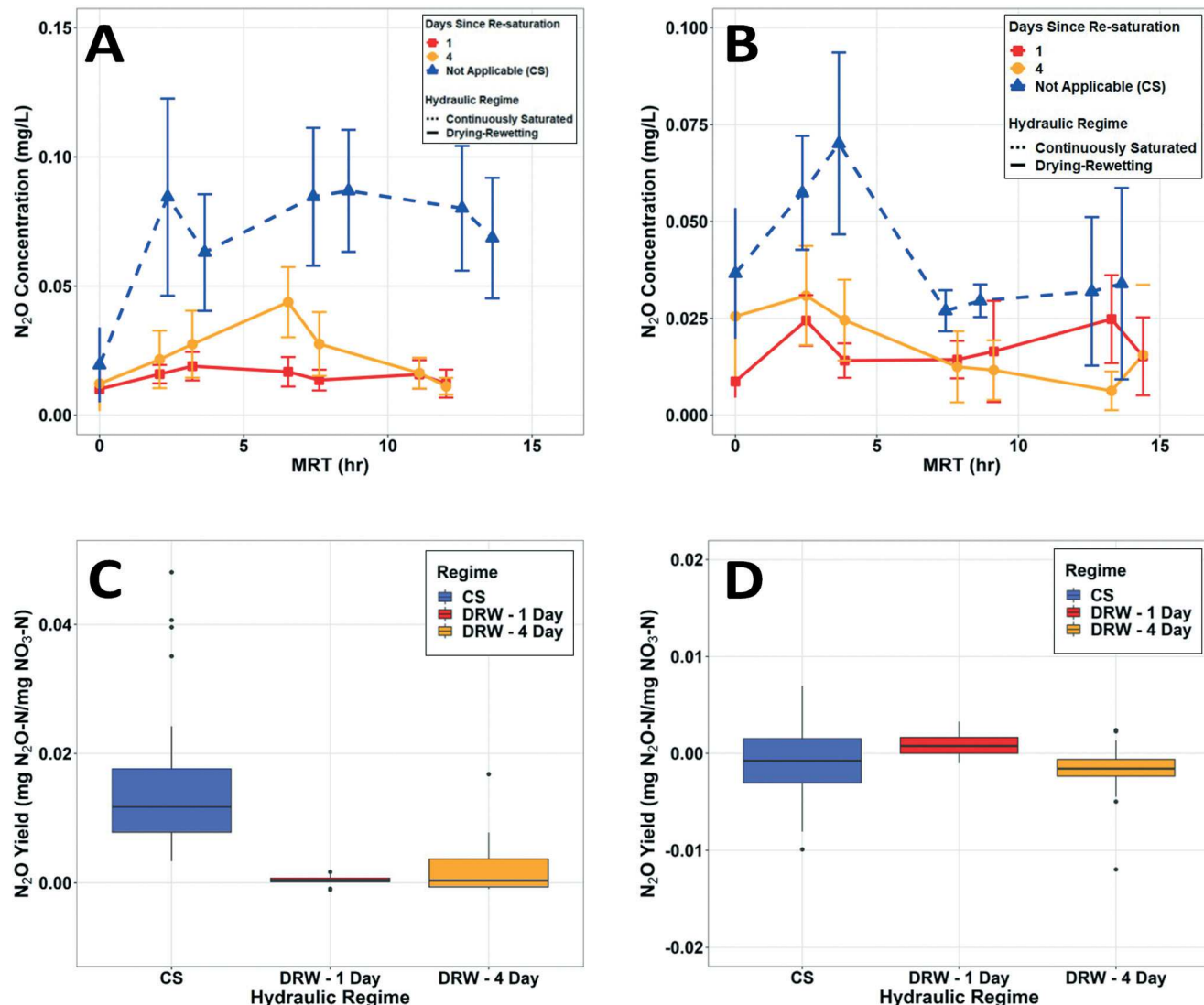


**Fig. 3** (A and B) Dissolved nitrous oxide (N<sub>2</sub>O) profiles in different hydraulic regimes. The x-axis represents distinct sampling ports, with mean residence time (MRT) determined as length along the reactor/porewater velocity. The differences in sample MRTs between CS and DRW reactors occurs because of slightly different hydraulic retention times in the two reactors. Symbols show mean values and error bars show standard deviation. (C and D) Effective N<sub>2</sub>O yields in downstream sampling ports (ports located at 0.86, 1.25, and 1.35 m), as defined in eqn (3). Panels (A) and (C) are from experiment 1. Panels (B) and (D) are from experiment 2.

removal rate 24 h following re-saturation and a 75% increase over the mean 96 h after re-saturation (Table 3). NO<sub>3</sub><sup>-</sup> removal rates were elevated immediately after re-saturation despite the presence of elevated DO in upstream portions of the reactor at those times (Fig. 5A), and week 6 was associated with a higher-than-usual DO concentration in the post re-saturation period. NO<sub>3</sub><sup>-</sup> removal rates in week 1 were generally lower than in following weeks and were the only instance in which there was not a clear decline in NO<sub>3</sub><sup>-</sup> removal rate as a function of time post re-saturation.

The effect of the oxic-anoxic transition on effective N<sub>2</sub>O yields changed over the course of the experiment. In weeks 1 and 3, N<sub>2</sub>O yields were positive in the period 4 to 10 h after re-flooding and declined as a function of time (Fig. 5C). This is consistent with the theory that transient microaerophilic

conditions inhibit N<sub>2</sub>O reduction and lead to higher N<sub>2</sub>O yields. However, in weeks 6 and 8, N<sub>2</sub>O yields exhibited a different pattern, with negative yields in the immediate post re-saturation period increasing over time before converging to yields similar to those observed in weeks 1 and 3 after 10 h. Notably, weeks 6 and 8 also had higher DO concentrations in this initial 10 h period than weeks 1 and 3 (Fig. 5A). The change in DIC ( $\Delta$ DIC) over the central portion of the reactor from 36 to 125 cm was examined to assess whether the negative N<sub>2</sub>O yields in weeks 6 and 8 were associated with signatures of greater C availability than weeks 1 and 3. Weeks 1, 6, and 8 were all characterized by an increase in  $\Delta$ DIC over time, indicating an increase in C respiration with time post re-saturation. However,  $\Delta$ DIC was not consistently greater in weeks 6 and 8 than week 1. Week 3 exhibited a different

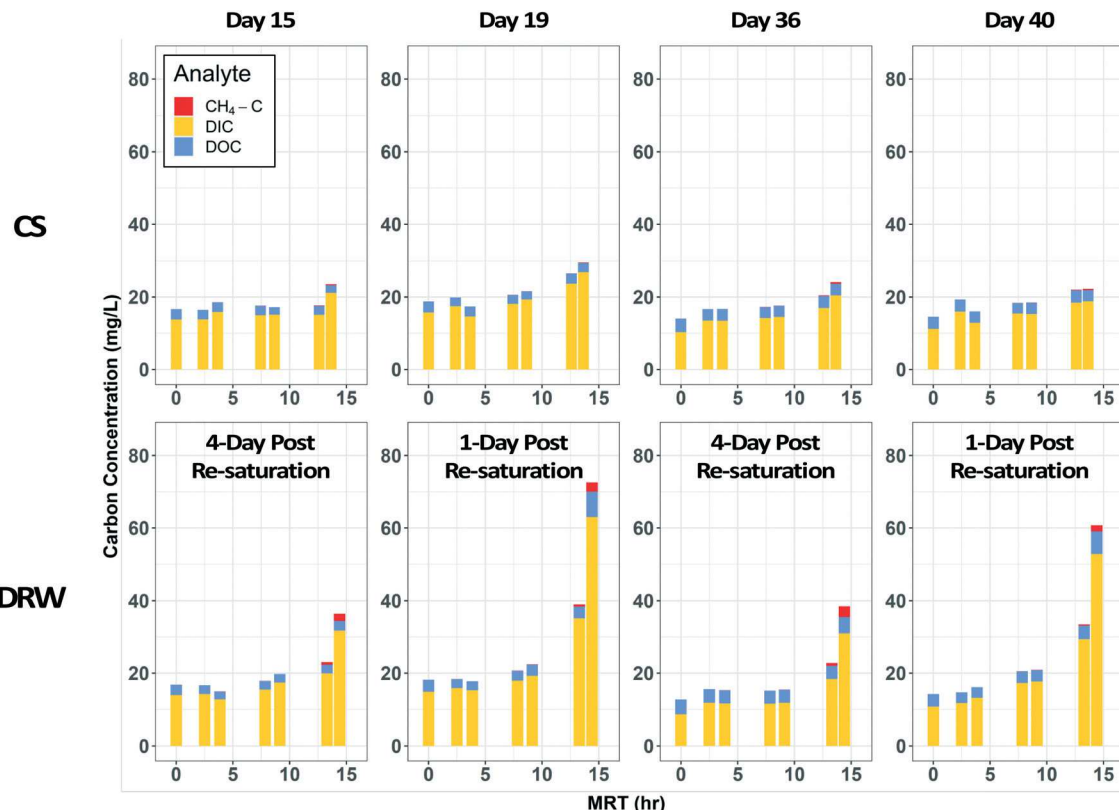


**Fig. 4** Profiles of dissolved inorganic carbon (DIC), dissolved organic carbon (DOC), and methane (CH<sub>4</sub>-C) from select sampling days in continuously saturated (CS) and drying-rewetting (DRW) reactors. Each bar represents a discrete water sampling port, with mean residence time (MRT) determined as length along the reactor/porewater velocity.

trend, with  $\Delta$ DIC beginning at a higher level than in the other weeks and decreasing with time. More post re-saturation data up to 80 h for weeks 3 and 6 as well as additional analysis of correlations among pore water solutes during oxic-anoxic transitions are available in the ESI† (Fig. S21–S28).

#### Batch reactor experiments

A follow-up set of batch reactor experiments was performed to complement flow-through reactor experiments and examine effects of antecedent oxic conditions on the quality of DOC mobilized from woodchips during subsequent anoxic periods. Woodchip media exposed to oxic-anoxic cycling demonstrated faster overall  $\text{NO}_3^-$  removal compared to the permanently anoxic reactor (Fig. 6A). The oxic-anoxic reactors (OAR) required fewer than 24 hours for complete  $\text{NO}_3^-$  removal while the anoxic reactors (AR) required at least 76 hours for complete  $\text{NO}_3^-$  removal.

Carbon release from the OARs greatly exceeded that of the ARs (Fig. 6B). After 125 hours, DOC concentrations in the OARs exceeded 100 mg C/L compared to concentrations in the ARs of approximately 30 mg C/L. Quantification of select low molecular weight organic acids (LMWOAs) revealed the dominant LMWOAs to be acetate and propionate. Butyrate was detected but contributed a negligible amount to total

DOC. Acetate concentrations began to increase in the OAR after 50 h, while in the AR acetate only began to increase in the final sample, after  $\text{NO}_3^-$  was fully depleted. Acetate comprised ~35% of the DOC in both the OARs and ARs in later timepoints, while propionate never exceeded 20% of the total DOC. SUVA analysis revealed a significantly lower aromaticity of the DOC pool in the OARs compared to ARs (Fig. 6C). In the OARs, SUVA declined by approximately 30% from hour 53 to 126 and was lower than SUVA in the ARs in all the measured samples. In the ARs, SUVA decreased by a factor of nearly 3 in the same timeframe from 2.75 L mg C<sup>-1</sup> m<sup>-1</sup> to 0.96 L mg C<sup>-1</sup> m<sup>-1</sup>.

## 4. Discussion

#### Effects of drying-rewetting cycles on carbon release and nitrate removal rates

This study confirms that DRW conditions significantly increase  $\text{NO}_3^-$  removal rates in WBRs. While this had been shown in some prior work,<sup>16,25,26,47</sup> a recent study, using a 54 h dry period in bench top WBRs, did not observe an increase in  $\text{NO}_3^-$  removal rates following repeated bioreactor DRW cycles.<sup>28</sup> The lack of a response may have been due to the use of relatively fresh woodchips and correspondingly high DOC levels even in the absence of DRW, or to  $\text{NO}_3^-$  limitation. Here, we show that  $\text{NO}_3^-$  removal rates were highest

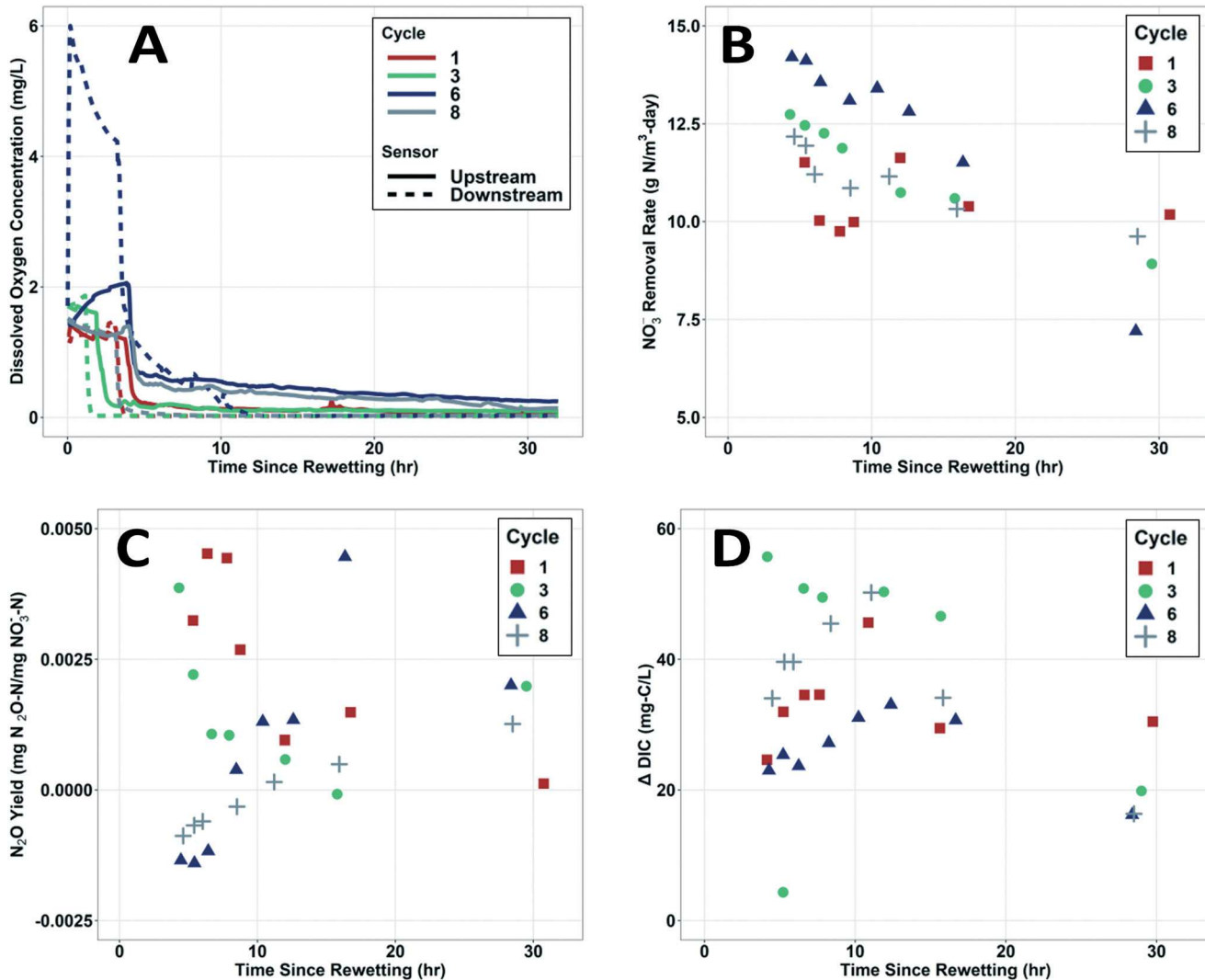


**Fig. 5** Porewater chemistry immediately following reactor rewetting during drying-rewetting (DRW) cycles 1, 3, 6, and 8. The x-axis represents the time of sampling relative to the re-flooding of the DRW reactor. The first samples were collected at roughly 5 h post re-saturation because it took 5 h for the water level to reach the sampling ports. Time 0 represents the start of rewetting. (A) Dissolved oxygen concentrations at upstream and downstream sensors; (B) nitrate removal rates; (C) effective nitrous oxide yields; (D) change in dissolved inorganic carbon ( $\Delta$ DIC) from sampling location at 36 to 125 cm at each time point.

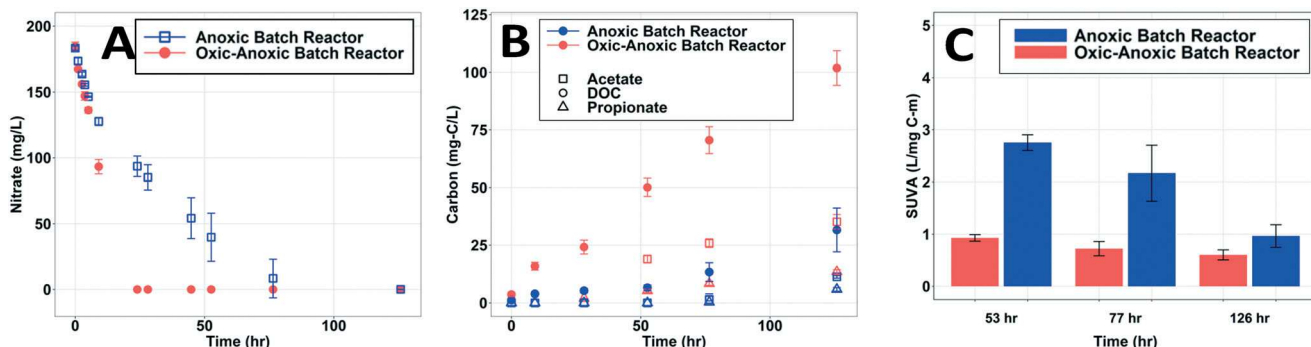


**Fig. 6** Aqueous nitrate removal and carbon quantity and quality in woodchip batch reactors conditioned under anoxic or oxic-anoxic conditions. At time 0, batch reactors were supplied with a fresh nutrient solution and all reactors were incubated anoxically. Symbols or bars show mean values and error bars show the standard deviation of  $n = 3$  reactors (A) nitrate removal; (B) mobilization of dissolved organic carbon and low molecular weight organic acids into solution; (C) specific ultraviolet absorbance (SUVA) at three different time points.

immediately after reactors were re-saturated and decreased from a maximum value of  $14.2 \text{ g N m}^{-3} \text{ d}^{-1}$  to  $8.1\text{--}9.6 \text{ g N m}^{-3} \text{ d}^{-1}$  four days after re-saturation. Mean  $\text{NO}_3^-$  removal rates in CS reactors were  $4.8\text{--}7.2 \text{ g N m}^{-3} \text{ d}^{-1}$ . These rates fall within the range of previously reported values for woodchip bioreactors.<sup>16,25</sup> For example, Maxwell *et al.* observed mean  $\text{NO}_3^-$  removal rates of  $12.3$  and  $8.9 \text{ g N m}^{-3} \text{ d}^{-1}$  for DRW and CS reactors, respectively.<sup>25</sup> Maxwell *et al.* used 8 h dry periods and observed that  $\text{NO}_3^-$  removal rates in DRW reactors remained higher than rates in CS reactors up to 7 d after reactor re-wetting.<sup>25</sup> Our study produced mixed results on the longevity of enhanced  $\text{NO}_3^-$  removal rates following a longer 48 h drainage period. In experiment 1,  $\text{NO}_3^-$  removal rates 4 d after the dry down were double the rates in the CS reactor, while in experiment 2 the mean rates in DRW-4 and CS were not significantly different. The lack of a significant difference between CS and DRW-4 in experiment 2 was largely due to a 50% increase in  $\text{NO}_3^-$  removal rates in the CS reactor between experiments 1 and 2. It is possible that the homogenization of woodchips between experiments contributed to this change, since half of the woodchips in the experiment 2 CS reactor had experienced DRW conditions in experiment 1, and the effects of antecedent DRW conditions on enhancing woodchip C release may have carried over into the experiment 2 CS reactor.  $\text{NO}_3^-$  profiles along the reactor in Experiment 2 exhibited a “kink” at an MRT of approximately 10 hours, which coincided with an increase of DOC and DIC, suggesting a potential role for C release processes in observed increases in  $\text{NO}_3^-$  removal rates in the latter portion of the column.

There was no evidence for elevated DO concentrations in the oxic-anoxic transition inhibiting  $\text{NO}_3^-$  reduction. The highest  $\text{NO}_3^-$  removal rates, usually observed in the first samples collected at roughly 5 h post re-saturation, sometimes had DO levels up to roughly  $0.5 \text{ mg L}^{-1}$  at the upstream DO sensor (Fig. 5A). While  $0.2\text{--}0.3 \text{ mg L}^{-1}$  is generally considered to be the  $\text{O}_2$  concentration threshold for the onset of denitrification,<sup>48</sup> in some aquifer systems this threshold could be as high as  $2 \text{ mg L}^{-1}$ .<sup>49,50</sup> It should be recognized however that the measured  $\text{O}_2$  concentrations in this system reflect the DO in the bulk porewater and more anoxic conditions will occur in the denitrifying biofilms. The highest  $\text{NO}_3^-$  removal rates in the oxic-anoxic transition were observed in week 6 (Fig. 5B), which corresponded to anomalously high DO concentrations at both upstream and downstream DO sensors. This DO anomaly is attributed to the removal of caps on woodchip sampling ports (Fig. S1†), for collecting woodchip samples for microbial analyses which will be reported in a forthcoming study.

Our study supports the theory that DRW conditions lead to faster  $\text{NO}_3^-$  removal rates by increasing soluble C mobilization from woodchips. Total carbon (TC) concentrations in the CS bioreactor of  $15\text{--}30 \text{ mg C/L}$  were similar to values reported elsewhere,<sup>25</sup> but concentrations in the DRW reactor effluent  $>60 \text{ mg C/L}$  were greater than those reported before. This may be due to the longer HRTs in our

systems (13–16 h) compared to HRTs in the prior study ( $8 \pm 2 \text{ h}$ ).<sup>23</sup> Increases in TC along the length of the DRW reactor were primarily driven by changes in DIC, with only small increases in DOC. This suggests that organic C mobilized from woodchips was quickly oxidized to  $\text{CO}_2$ . The increase in ADIC with time after re-saturation observed during most weeks (Fig. 5D) suggests that respiration increased as more  $\text{NO}_3^-$  – rich floodwater flowed through the woodchip media. A notable result in this study was the observation of dissolved  $\text{CH}_4$  in the DRW reactors, while concentrations in the CS reactors were negligible. The presence of  $\text{CH}_4$  in the bulk fluid one day after re-saturation, and in water samples containing  $\text{NO}_3^-$  (Fig. 2A), points to microbial activity in deeply reducing microenvironments in woodchip-attached biofilms or inside the woodchip<sup>51</sup> in DRW conditions. The lack of DIC and/or  $\text{CH}_4$  accumulation in the DRW reactors before the final two water sample points may be due in part to the presence of a headspace in woodchip sampling ports upstream of the final water sample points that could harbor a reservoir of  $\text{CO}_2$  or  $\text{CH}_4$  (Fig. S1 and S2†).

Batch experiments provided further support for links between antecedent oxic conditions, greater organic C mobilization from woodchips, and faster  $\text{NO}_3^-$  removal rates. Woodchips in the oxic-anoxic reactor released roughly three times as much DOC as the woodchips in the anoxic reactor. There was a notable difference in the aromaticity of the soluble organic carbon pool between the oxic-anoxic and anoxic reactors. Lignin is a phenolic heteropolymer, so the aromatic dissolved C fraction in the bioreactors is most probably derived from lignin. The lower aromaticity in the oxic-anoxic reactor therefore reflects (a) greater oxidative ring-opening of aromatic structures and/or (b) a greater contribution of cellulose- or hemicellulose-derived carbon. Both cases are consistent with the theory that antecedent oxic conditions unlock labile fractions of woodchip carbon.

### Effects of drying–rewetting cycles on nitrous oxide

We originally hypothesized that drying–rewetting cycles would increase  $\text{N}_2\text{O}$  production in WBRs, particularly in the transition from oxic to anoxic conditions, due to  $\text{O}_2$  inhibition of NosZ enzymes. We recently showed that the internal pores of woodchips harbor trapped gas phases after water levels rise in woodchip bioreactors,<sup>52</sup> suggesting that  $\text{O}_2$  may persist inside woodchips after it is depleted in the bulk fluid and underscoring the potential for drying–rewetting events to lead to microaerophilic conditions inside reactors. Interpretation of differences in  $\text{N}_2\text{O}$  concentrations within WBRs was complicated by non-zero levels of  $\text{N}_2\text{O}$  in the reactor influent (Fig. 3A and B). This may have resulted from nitrification of  $\text{NH}_4^+$  in the reactor influent and was not intentional, but it does represent field conditions, where  $\text{N}_2\text{O}$  produced in soils or in tile drains is introduced to bioreactors.<sup>53</sup> Because of this, we used effective  $\text{N}_2\text{O}$  yields to evaluate the effects of drying–rewetting treatments on  $\text{N}_2\text{O}$  dynamics, since this accounted for the change in  $\text{N}_2\text{O}$

concentrations relative to the influent (eqn (3)). Results from 1 and 4 days post re-saturation showed that our original hypothesis was not correct.  $\text{N}_2\text{O}$  yields were either lower (experiment 1) or not different (experiment 2) in DRW reactors compared to CS reactors (Fig. 3C and D). One explanation for lower  $\text{N}_2\text{O}$  yields is that greater C availability accelerated microbial  $\text{N}_2\text{O}$  reduction along with faster  $\text{NO}_3^-$  reduction, as has been postulated by Feyereisen *et al.*<sup>23</sup> While our previous work suggested that water level draw-downs could release  $\text{N}_2\text{O}$  held in trapped gas phases,<sup>52</sup> we did not observe this here based on occasional measurements of bioreactor air (data not shown).

Data from the oxic–anoxic transition showed that in weeks 1 and 3 there was a transient increase in  $\text{N}_2\text{O}$  yields in the first hours after re-saturation that decreased with time and decreasing DO, consistent with our expectation. However, by weeks 6 and 8 this pattern reversed, and the immediate post re-saturation period was characterized by low  $\text{N}_2\text{O}$  yields that increased with time and decreasing DO. This difference between early and late phases of the experiment was not explained by differences in DO, since DO concentrations were higher in weeks 6 and 8 than 1 and 3 (Fig. 5A). One plausible explanation would be that greater C release in the immediate post re-saturation phase of weeks 6 and 8 accelerated  $\text{N}_2\text{O}$  reduction despite higher DO, perhaps due to a cumulative effect of bioreactor drainage events, but evidence for this is mixed. Weeks 6 and 8 do not exhibit systematically higher  $\Delta\text{DIC}$  than weeks 1 and 3 in the post re-saturation phase (Fig. 5D and S36†). However, week 8 does exhibit significantly higher DOC than all other weeks and week 6 exhibits significantly higher DOC concentrations than week 1 (Fig. S35†). The difference in  $\text{N}_2\text{O}$  yields in the immediate post re-saturation between weeks 3 and 6 does not persist after 20 h (Fig. S23†). While Fig. 5C does reveal that oxic–anoxic transitions may at times lead to transient increases in  $\text{N}_2\text{O}$  yields, a Kruskal–Wallis rank sum test showed that the mean  $\text{N}_2\text{O}$  yields in the period up to 30 h after re-saturation in weeks 1 and 3 were not significantly greater than the  $\text{N}_2\text{O}$  yields measured in the CS reactor ( $p = 0.092$ ).

This is among the first studies to evaluate the impact of drying–rewetting conditions on  $\text{N}_2\text{O}$  dynamics in WBRs. Manca *et al.* recently evaluated  $\text{N}_2\text{O}$  dynamics in WBRs experiencing drying–rewetting cycles and showed that dissolved  $\text{N}_2\text{O}$  concentrations in bench-top WBRs were higher 1 day after re-saturation compared to 3 and 5 days after re-saturation.<sup>28</sup> They did not compare their results in DRW reactors to data in continuously saturated reactors, so the overall effect of DRW cycles on  $\text{N}_2\text{O}$  dynamics was difficult to assess. Our study did not show that DRW cycling increased  $\text{N}_2\text{O}$  yields compared to CS reactors 1 or 4 days post re-saturation, most probably due to greater carbon availability in DRW reactors.

The lack of significant enhancement in  $\text{N}_2\text{O}$  accumulation in the transition from oxic to anoxic conditions indicates that greater C availability outweighs inhibitory effects of  $\text{O}_2$  and/or that  $\text{O}_2$  inhibition of  $\text{N}_2\text{O}$  reduction was minor or short-

lived. DO concentrations as low as  $0.6 \text{ mg L}^{-1}$  have been shown to significantly inhibit  $\text{N}_2\text{O}$  reduction rates by up to 90% in numerous bacterial strains, with some strains unable to reduce  $\text{N}_2\text{O}$  until DO was completely depleted.<sup>54</sup> DO concentrations at the upstream sensor of the WBRs were in this range up to 10 h after re-saturation in weeks 6 and 8, and in week 6 the downstream sensor position was also characterized by DO concentrations in this range (Fig. 5A). Notably, weeks 6 and 8 were also characterized by the lowest  $\text{N}_2\text{O}$  yields, with reactors acting as an  $\text{N}_2\text{O}$  sink (negative  $\text{N}_2\text{O}$  yields) in several cases (Fig. 5C). So, there was no clear evidence of a link between microaerophilic  $\text{O}_2$  levels and inhibited  $\text{N}_2\text{O}$  reduction in the oxic–anoxic transition even though DO levels observed in the bioreactor have been associated with inhibited  $\text{N}_2\text{O}$  reduction elsewhere. Prior studies have shown that  $\text{N}_2\text{O}$ -reducing microorganisms recover most of their  $\text{N}_2\text{O}$  reducing activity within 1–4 h after  $\text{O}_2$  has been depleted,<sup>54,55</sup> and this relatively fast recovery may contribute to the lack of  $\text{N}_2\text{O}$  accumulation during the oxic–anoxic transition. While there have been investigations into the microbial community of denitrifying woodchip bioreactors in recent years,<sup>20,56–58</sup> there has been little focused study of the  $\text{N}_2\text{O}$ -reducing community, so it is not clear how well the results of pure culture studies translate to the bioreactor community.

### Implications for field operation of woodchip bioreactors

This study suggests that implementation of DRW cycles in woodchip bioreactors has the potential to increase  $\text{NO}_3^-$  removal rates without increasing  $\text{N}_2\text{O}$  production, and that DRW cycles may, in fact, diminish  $\text{N}_2\text{O}$  production compared to traditional, continuously saturated conditions. With recent innovations in “smart” water infrastructure,<sup>59–61</sup> cost-effective capabilities for automating drying and rewetting of woodchip bioreactors based on sensor feedbacks or precipitation forecasting are in reach. A key need for future research is to determine the optimal duration of dry periods and periodicity of drying–rewetting cycles so as to maximize  $\text{NO}_3^-$  removal rates while minimizing dry periods when water will be discharged directly to surface waters without treatment. The 8 h dry periods used in Maxwell *et al.*<sup>25</sup> resulted in comparable increases in  $\text{NO}_3^-$  removal rate as the 48 h dry periods tested in this study, suggesting that marginal increases in carbon release with time may be small and that shorter dry periods may be optimal.<sup>25</sup> However, in a separate study, Maxwell *et al.*<sup>16</sup> found that increased durations of 2, 8, and 24 hour drying periods during a weekly cycle produced dramatically higher  $\text{NO}_3^-$  removal rates with longer unsaturated periods.<sup>16</sup> The effect of the duration of unsaturated periods on C release, and its interaction with variables including woodchip age, temperature,<sup>45</sup> and water chemistry, thus remain unclear and merit further attention. Effects of DRW management on  $\text{N}_2\text{O}$  dynamics are also likely to be temperature-dependent, since  $\text{N}_2\text{O}$  reduction rates are thought to be more temperature-sensitive than the reduction

## Paper

Published on 13 October 2021. Downloaded by Cornell University Library on 11/1/2021 1:39:58 PM.

rates of upstream nitrogen oxide species.<sup>62</sup> While evaluating effects of HRT variability on N<sub>2</sub>O yields was beyond the scope of this study, HRT is a critical determinant on WBR N dynamics<sup>63–65</sup> and other processes.<sup>67</sup> N<sub>2</sub>O measurements from experiment 1 in particular support a conceptual model of net N<sub>2</sub>O production followed by net N<sub>2</sub>O consumption,<sup>66</sup> so it is probable that shorter HRTs could lead to greater N<sub>2</sub>O yields if the system effluent is shifted towards the net N<sub>2</sub>O production regime.

Implementation of DRW management of WBRs will most likely accelerate the depletion of the woodchip media and reduce the effective lifetime of WBRs.<sup>13</sup> Woodchip replacement may significantly contribute to the life cycle cost of WBRs,<sup>68</sup> though reports of woodchip replacement costs in the literature are limited. More research is needed to determine the economic trade-offs, from the perspective of life cycle cost per unit NO<sub>3</sub><sup>–</sup> removed, incurred by woodchip media replacement. Another concern associated with DRW practices is the direct release of untreated tile drainage during drained periods, but this could be addressed by building parallel bioreactors so that one is always available for treatment.

Optimizing the benefits of DRW cycling for NO<sub>3</sub><sup>–</sup> removal also requires further investigation into the biogeochemical mechanisms driving faster C mobilization from woodchips in DRW conditions. Our study produced novel results that antecedent oxic periods lead to a water-soluble organic C pool with lower aromaticity than a permanently anoxic reactor, highlighting the importance of lignin breakdown and liberation of cellulose and hemicellulose for WBR performance. Fungi are the primary drivers of lignocellulose breakdown in the environment, through oxygen-dependent enzymes or production of reactive oxygen species *via* Fenton reactions.<sup>69</sup> Both of these pathways would be enhanced by alternating oxic-anoxic conditions in bioreactors. Fungal bioaugmentation could therefore be an important strategy for optimizing WBR performance under DRW cycling. Augmentation with manganese (Mn) may also serve an important role, since Mn has been shown to regulate rates of lignocellulose decay,<sup>70,71</sup> presumably due to the role of manganese peroxidase enzymes in lignin breakdown. These processes will require focused study in the context of denitrifying woodchip bioreactors before recommendations on how to optimize reactor biological and chemical properties for enhanced breakdown of lignocellulosic carbon can be made.

## Author contributions

Conceptualization – PMM, MCR, MTW; data curation – VD, PMM, MCR; formal analysis – PMM, MCR; funding acquisition – PMM, MCR, MTW; investigation – VD, PMM; MCR Methodology – PMM, MCR, MTW; project administration – PMM, MCR, MTW; resources – MCR, MTW; software – VD, PMM, MCR; supervision – PMM, MCR, MTW; validation – VD, PMM, MCR; visualization – VD, PMM, MCR; writing – original draft – PMM, MCR; writing – review & editing – PMM, MCR, MTW.

## Conflicts of interest

There are no conflicts to declare.

## Acknowledgements

This research was funded by NSF award number 1804975. Additional funding was provided by the Cornell Rawlings Presidential Research Scholars Program. The authors thank C. Peterson for assistance with reactor construction, and L. Hurt, V. Starnes, and J. Israel for assistance with bioreactor sampling and maintenance.

## References

- 1 L. E. Christianson, R. A. Cooke, C. H. Hay, M. J. Helmers, G. W. Feyereisen, A. Z. Ranaivoson, J. T. McMaine, R. McDaniel, T. R. Rosen and W. T. Pluer, *et al.*, Effectiveness of Denitrifying Bioreactors on Water Pollutant Reduction from Agricultural Areas, *Trans. ASABE*, 2021, 641–658, DOI: 10.13031/TRANS.14011.
- 2 E. V. Lopez, T. J. Lynn, M. Peterson, S. J. Ergas, M. A. Trotz and J. R. Mihelcic, Enhanced Nutrient Management of Stormwater through a Field Demonstration of Nitrogen Removal in a Modified Bioretention System, in *World Environmental And Water Resources Congress 2016: Environmental, Sustainability, Groundwater, Hydraulic Fracturing, and Water Distribution Systems Analysis - Papers from Sessions of the Proceedings of the 2016 World Environmental and Water Resources*, 2016, DOI: 10.1061/9780784479865.007.
- 3 C. C. Tanner, J. P. S. Sukias, T. R. Headley, C. R. Yates and R. Stott, Constructed Wetlands and Denitrifying Bioreactors for On-Site and Decentralised Wastewater Treatment: Comparison of Five Alternative Configurations, *Ecol. Eng.*, 2012, **42**, 112–123, DOI: 10.1016/j.ecoleng.2012.01.022.
- 4 Institute for Environment and Sustainability (Joint Research Centre), *Managing Nitrogen and Phosphorus Loads to Water Bodies-Characterisation and Solutions: Towards Macro-Regional Integrated Nutrient Management*, 2014, DOI: 10.2788/14322.
- 5 S. Warneke, L. A. Schipper, M. G. Matiasek, K. M. Scow, S. Cameron, D. A. Bruesewitz and I. R. McDonald, Nitrate Removal, Communities of Denitrifiers and Adverse Effects in Different Carbon Substrates for Use in Denitrification Beds, *Water Res.*, 2011, **45**(17), 5463–5475, DOI: 10.1016/j.watres.2011.08.007.
- 6 R. Hu, X. Zheng, T. Zheng, J. Xin, H. Wang and Q. Sun, Effects of Carbon Availability in a Woody Carbon Source on Its Nitrate Removal Behavior in Solid-Phase Denitrification, *J. Environ. Manage.*, 2019, **246**, 832–839, DOI: 10.1016/j.jenvman.2019.06.057.
- 7 M. B. Roser, G. W. Feyereisen, K. A. Spokas, D. J. Mulla, J. S. Strock and J. Gutknecht, Carbon Dosing Increases Nitrate Removal Rates in Denitrifying Bioreactors at Low-Temperature High-Flow Conditions, *J. Environ. Qual.*, 2018, **47**(4), 856–864, DOI: 10.2134/jeq2018.02.0082.
- 8 I. Abusallout and G. Hua, Characterization of Dissolved Organic Carbon Leached from a Woodchip Bioreactor,

*Chemosphere*, 2017, **183**, 36–43, DOI: 10.1016/j.chemosphere.2017.05.066.

9 R. D. DeLaune, R. R. Boar, C. W. Lindau and B. A. Kleiss, Denitrification in Bottomland Hardwood Wetland Soils of the Cache River, *Wetlands*, 1996, **16**(3), 309–320, DOI: 10.1007/BF03161322.

10 N. P. Hume, M. S. Fleming and A. J. Horne, Denitrification Potential and Carbon Quality of Four Aquatic Plants in Wetland Microcosms, *Soil Sci. Soc. Am. J.*, 2002, **66**(5), 1706–1712, DOI: 10.2136/sssaj2002.1706.

11 S. Warneke, L. A. Schipper, D. A. Bruesewitz and W. T. Baisden, A Comparison of Different Approaches for Measuring Denitrification Rates in a Nitrate Removing Bioreactor, *Water Res.*, 2011, **45**(14), 4141–4151, DOI: 10.1016/j.watres.2011.05.027.

12 A. Kouanda and G. Hua, Determination of Nitrate Removal Kinetics Model Parameters in Woodchip Bioreactors, *Water Res.*, 2021, **195**, 116974, DOI: 10.1016/j.watres.2021.116974.

13 T. B. Moorman, T. B. Parkin, T. C. Kaspar and D. B. Jaynes, Denitrification Activity, Wood Loss, and N<sub>2</sub>O Emissions over 9 Years from a Wood Chip Bioreactor, *Ecol. Eng.*, 2010, **36**, 1567–1574, DOI: 10.1016/j.ecoleng.2010.03.012.

14 M. B. David, L. E. Gentry, R. A. Cooke and S. M. Herbstritt, Temperature and Substrate Control Woodchip Bioreactor Performance in Reducing Tile Nitrate Loads in East-Central Illinois, *J. Environ. Qual.*, 2016, **45**(3), 822–829, DOI: 10.2134/jeq2015.06.0296.

15 E. Ghane, G. W. Feyereisen, C. J. Rosen and U. W. Tschirner, Carbon Quality of Four-Year-Old Woodchips in a Denitrification Bed Treating Agricultural Drainage Water, *Trans. ASABE*, 2018, **61**(3), 995–1000, DOI: 10.13031/trans.12642.

16 B. M. Maxwell, F. Birgand, L. A. Schipper, L. E. Christianson, S. Tian, M. J. Helmers, D. J. Williams, G. M. Chescheir and M. A. Youssef, Increased Duration of Drying–Rewetting Cycles Increases Nitrate Removal in Woodchip Bioreactors, *Agric. Environ. Lett.*, 2019, **4**(1), 190028, DOI: 10.2134/ael2019.07.0028.

17 B. J. Halaburka, G. H. Lefevre and R. G. Luthy, Evaluation of Mechanistic Models for Nitrate Removal in Woodchip Bioreactors, *Environ. Sci. Technol.*, 2017, **51**(9), 5156–5164, DOI: 10.1021/acs.est.7b01025.

18 W. D. Robertson, Nitrate Removal Rates in Woodchip Media of Varying Age, *Ecol. Eng.*, 2010, **36**(11), 1581–1587, DOI: 10.1016/j.ecoleng.2010.01.008.

19 Y. Pan, B. J. Ni, P. L. Bond, L. Ye and Z. Yuan, Electron Competition among Nitrogen Oxides Reduction during Methanol-Utilizing Denitrification in Wastewater Treatment, *Water Res.*, 2013, **47**(10), 3273–3281, DOI: 10.1016/j.watres.2013.02.054.

20 S. L. Aalto, S. Suurnäkki, M. von Ahnen, H. M. P. Siljanen, P. B. Pedersen and M. Tiirola, Nitrate Removal Microbiology in Woodchip Bioreactors: A Case-Study with Full-Scale Bioreactors Treating Aquaculture Effluents, *Sci. Total Environ.*, 2020, **723**, 138093, DOI: 10.1016/j.scitotenv.2020.138093.

21 A. R. Ravishankara, J. S. Daniel and R. W. Portmann, Nitrous Oxide (N<sub>2</sub>O): The Dominant Ozone-Depleting Substance Emitted in the 21st Century, *Science*, 2009, **326**(5949), 123–125, DOI: 10.1126/science.1176985.

22 M. B. Roser, G. W. Feyereisen, K. A. Spokas, D. J. Mulla, J. S. Strock and J. Gutknecht, Carbon Dosing Increases Nitrate Removal Rates in Denitrifying Bioreactors at Low-Temperature High-Flow Conditions, *J. Environ. Qual.*, 2018, **47**(4), 856–864, DOI: 10.2134/jeq2018.02.0082.

23 G. W. Feyereisen, K. A. Spokas, J. S. Strock, D. J. Mulla, A. Z. Ranaivoson and J. A. Coulter, Nitrate Removal and Nitrous Oxide Production from Upflow and Downflow Column Woodchip Bioreactors, *Agric. Environ. Lett.*, 2020, **5**(1), e20024, DOI: 10.1002/ael2.20024.

24 S. Jansen, R. Stuurman, W. Chardon, S. Ball, J. Rozemeijer and J. Gerritsse, Passive Dosing of Organic Substrates for Nitrate-Removing Bioreactors Applied in Field Margins, *J. Environ. Qual.*, 2019, **48**(2), 394–402, DOI: 10.2134/jeq2018.04.0165.

25 B. M. Maxwell, F. Birgand, L. A. Schipper, L. E. Christianson, S. Tian, M. J. Helmers, D. J. Williams, G. M. Chescheir and M. A. Youssef, Drying–Rewetting Cycles Affect Nitrate Removal Rates in Woodchip Bioreactors, *J. Environ. Qual.*, 2019, **48**(1), 93–101, DOI: 10.2134/jeq2018.05.0199.

26 B. M. Maxwell, C. Diáz-García, J. J. Martínez-Sánchez, F. Birgand and J. Álvarez-Rogel, Temperature Sensitivity of Nitrate Removal in Woodchip Bioreactors Increases with Woodchip Age and Following Drying–Rewetting Cycles, *Environ. Sci.: Water Res. Technol.*, 2020, **6**(10), 2752–2765, DOI: 10.1039/d0ew00507j.

27 L. E. Christianson, C. Lepine, P. L. Sibrell, C. Penn and S. T. Summerfelt, Denitrifying Woodchip Bioreactor and Phosphorus Filter Pairing to Minimize Pollution Swapping, *Water Res.*, 2017, **121**, 129–139, DOI: 10.1016/j.watres.2017.05.026.

28 F. Manca, D. De Rosa, L. P. Reading, D. W. Rowlings, C. Scheer, L. A. Schipper and P. R. Grace, Effect of Soil Cap and Nitrate Inflow on Nitrous Oxide Emissions from Woodchip Bioreactors, *Ecol. Eng.*, 2021, **166**, 106235, DOI: 10.1016/j.ecoleng.2021.106235.

29 X. Guo, C. F. Drury, X. Yang, W. D. Reynolds and R. Fan, The Extent of Soil Drying and Rewetting Affects Nitrous Oxide Emissions, Denitrification, and Nitrogen Mineralization, *Soil Sci. Soc. Am. J.*, 2014, **78**(1), 194–204, DOI: 10.2136/SSAJ2013.06.0219.

30 H. Arai, M. Mizutani and Y. Igarashi, Transcriptional Regulation of the Nos Genes for Nitrous Oxide Reductase in *Pseudomonas aeruginosa*, *Microbiology*, 2003, **149**(1), 29–36, DOI: 10.1099/mic.0.25936-0.

31 H. Korner and W. G. Zumft, Expression of Denitrification Enzymes in Response to the Dissolved Oxygen Levels and Respiratory Substrate in Continuous Culture of *Pseudomonas stutzeri*, *Appl. Environ. Microbiol.*, 1989, **55**(7), 1670–1676, DOI: 10.1128/aem.55.7.1670-1676.1989.

32 W. G. Zumft, Cell Biology and Molecular Basis of Denitrification, *Microbiol. Mol. Biol. Rev.*, 1997, **61**(4), 533–616.

33 B. J. Ni, M. Ruscalleda, C. Pellicer-Nàcher and B. F. Smets, Modeling Nitrous Oxide Production during Biological Nitrogen Removal via Nitrification and Denitrification:

## Paper

## Environmental Science: Water Research &amp; Technology

Extensions to the General ASM Models, *Environ. Sci. Technol.*, 2011, **45**(18), 7768–7776, DOI: 10.1021/es201489n.

34 A. Pandey, V. T. Mai, D. Q. Vu, T. P. L. Bui, T. L. A. Mai, L. S. Jensen and A. de Neergaard, Organic Matter and Water Management Strategies to Reduce Methane and Nitrous Oxide Emissions from Rice Paddies in Vietnam, *Agric., Ecosyst. Environ.*, 2014, **196**, 137–146, DOI: 10.1016/j.agee.2014.06.010.

35 B. A. Linquist, M. M. Anders, M. A. A. Adviento-Borbe, R. L. Chaney, L. L. Nalley, E. F. F. da Rosa and C. van Kessel, Reducing Greenhouse Gas Emissions, Water Use, and Grain Arsenic Levels in Rice Systems, *Glob. Chang. Biol.*, 2015, **21**(1), 407–417, DOI: 10.1111/gcb.12701.

36 B. Hassanpour, S. Giri, W. T. Pluer, T. S. Steenhuis and L. D. Geohring, Seasonal Performance of Denitrifying Bioreactors in the Northeastern United States: Field Trials, *J. Environ. Manage.*, 2017, **202**(1), 242–253, DOI: 10.1016/j.jenvman.2017.06.054.

37 E. Ghane, G. W. Feyereisen and C. J. Rosen, Efficacy of Bromide Tracers for Evaluating the Hydraulics of Denitrification Beds Treating Agricultural Drainage Water, *J. Hydrol.*, 2019, **574**, 129–137, DOI: 10.1016/j.jhydrol.2019.02.031.

38 J. M. Simunek, M. Th. van Genuchten, N. Toride Sejna and F. J. Leij, *The STANMOD Computer Software for Evaluating Solute Transport in Porous Media Using Analytical Solutions of Convection-Dispersion Equation, Versions 1.0 and 2.0*, U.S. Salinity Laboratory, USDA, ARS, Riverside, California, 1999.

39 M. T. Van Genuchten, J. Šimůnek, F. J. Leij, N. Toride and M. Šejna, STANMOD: Model Use, Calibration, and Validation, *Trans. ASABE*, 2012, **55**(4), 1353–1366.

40 M. E. McClain, E. W. Boyer, C. L. Dent, S. E. Gergel, N. B. Grimm, P. M. Groffman, S. C. Hart, J. W. Harvey, C. A. Johnston and E. Mayorga, *et al.*, Biogeochemical Hot Spots and Hot Moments at the Interface of Terrestrial and Aquatic Ecosystems, *Ecosystems*, 2003, **6**(4), 301–312, DOI: 10.1007/s10021-003-0161-9.

41 P. M. Groffman, K. Butterbach-Bahl, R. W. Fulweiler, A. J. Gold, J. L. Morse, E. K. Stander, C. Tague, C. Tonitto and P. Vidon, Challenges to Incorporating Spatially and Temporally Explicit Phenomena (Hotspots and Hot Moments) in Denitrification Models, *Biogeochemistry*, 2009, **93**, 49–77, DOI: 10.1007/s10533-008-9277-5.

42 F. M. M. Morel and J. G. Hering, *Principles and Applications of Aquatic Chemistry*, John Wiley & Sons, 1993.

43 J. L. Weishaar, G. R. Aiken, B. A. Bergamaschi, M. S. Fram, R. Fujii and K. Mopper, Evaluation of Specific Ultraviolet Absorbance as an Indicator of the Chemical Composition and Reactivity of Dissolved Organic Carbon, *Environ. Sci. Technol.*, 2003, **37**(20), 4702–4708, DOI: 10.1021/es030360x.

44 R Core Team, *R: A Language and Environment for Statistical Computing*, 2021, DOI: 10.1007/978-3-540-74686-7.

45 B. J. Halaburka, G. H. Lefevre and R. G. Luthy, Quantifying the Temperature Dependence of Nitrate Reduction in Woodchip Bioreactors: Experimental and Modeled Results with Applied Case-Study, *Environ. Sci.: Water Res. Technol.*, 2019, **5**(4), 782–797, DOI: 10.1039/c8ew00848e.

46 S. Warneke, L. A. Schipper, D. A. Bruesewitz, I. McDonald and S. Cameron, Rates, Controls and Potential Adverse Effects of Nitrate Removal in a Denitrification Bed, *Ecol. Eng.*, 2011, **37**(3), 511–522, DOI: 10.1016/j.ecoleng.2010.12.006.

47 G. Hua, M. W. Salo, C. G. Schmit and C. H. Hay, Nitrate and Phosphate Removal from Agricultural Subsurface Drainage Using Laboratory Woodchip Bioreactors and Recycled Steel Byproduct Filters, *Water Res.*, 2016, **102**, 180–189, DOI: 10.1016/j.watres.2016.06.022.

48 S. Seitzinger, J. A. Harrison, J. K. Böhlke, A. F. Bouwman, R. Lowrance, B. Peterson, C. Tobias and G. Van Drecht, Denitrification across Landscapes and Waterscapes: A Synthesis, *Ecol. Appl.*, 2006, 2064–2090, DOI: 10.1890/1051-0761(2006)016[2064:DALAWA]2.0.CO;2.

49 P. B. McMahon, J. K. Böhlke and S. C. Christenson, Geochemistry, Radiocarbon Ages, and Paleorecharge Conditions along a Transect in the Central High Plains Aquifer, Southwestern Kansas, USA, *Appl. Geochem.*, 2004, **19**(11), 1655–1686, DOI: 10.1016/J.APGEOCHEM.2004.05.003.

50 J. K. Böhlke, R. Wanty, M. Tuttle, G. Delin and M. Landon, Denitrification in the Recharge Area and Discharge Area of a Transient Agricultural Nitrate Plume in a Glacial Outwash Sand Aquifer Minnesota, *Water Resour. Res.*, 2002, **38**(7), 10–11, DOI: 10.1029/2001WR000663.

51 E. V. Lopez-Ponnada, T. J. Lynn, M. Peterson, S. J. Ergas and J. R. Mihelcic, Application of Denitrifying Wood Chip Bioreactors for Management of Residential Non-Point Sources of Nitrogen, *J. Biol. Eng.*, 2017, **11**, DOI: 10.1186/s13036-017-0057-4.

52 P. M. McGuire and M. C. Reid, Nitrous Oxide and Methane Dynamics in Woodchip Bioreactors: Effects of Water Level Fluctuations on Partitioning into Trapped Gas Phases, *Environ. Sci. Technol.*, 2019, **53**(24), 14348–14356, DOI: 10.1021/acs.est.9b04829.

53 M. P. Davis, E. A. Martin, T. B. Moorman, T. M. Isenhart and M. L. Soupir, Nitrous Oxide and Methane Production from Denitrifying Woodchip Bioreactors at Three Hydraulic Residence Times, *J. Environ. Manage.*, 2019, **242**, 290–297, DOI: 10.1016/j.jenvman.2019.04.055.

54 T. Suenaga, S. Riya, M. Hosomi and A. Terada, Biokinetic Characterization and Activities of N<sub>2</sub>O-Reducing Bacteria in Response to Various Oxygen Levels, *Front. Microbiol.*, 2018, **9**, 697, DOI: 10.3389/fmicb.2018.00697.

55 Y. Zhou, T. Suenaga, C. Qi, S. Riya, M. Hosomi and A. Terada, Temperature and Oxygen Level Determine N<sub>2</sub>O Respiration Activities of Heterotrophic N<sub>2</sub>O-Reducing Bacteria: Biokinetic Study, *Biotechnol. Bioeng.*, 2021, **118**(3), 1330–1341, DOI: 10.1002/bit.27654.

56 J. Jang, E. L. Anderson, R. T. Venterea, M. J. Sadowsky, C. J. Rosen, G. W. Feyereisen and S. Ishii, Denitrifying Bacteria Active in Woodchip Bioreactors at Low-Temperature Conditions, *Front. Microbiol.*, 2019, **10**, 635, DOI: 10.3389/fmicb.2019.00635.

57 D. van der Lelie, S. Taghavi, S. M. McCorkle, L. L. Li, S. A. Malfatti, D. Monteleone, B. S. Donohoe, S. Y. Ding, W. S. Adney and M. E. Himmel, *et al.*, The Metagenome of an Anaerobic Microbial Community Decomposing Poplar Wood

Chips, *PLoS One*, 2012, **7**(5), e36740, DOI: 10.1371/journal.pone.0036740.

58 M. Hellman, V. Hubalek, J. Juhanson, R. Almstrand, S. Peura and S. Hallin, Substrate Type Determines Microbial Activity and Community Composition in Bioreactors for Nitrate Removal by Denitrification at Low Temperature, *Sci. Total Environ.*, 2021, **755**, 143023, DOI: 10.1016/j.scitotenv.2020.143023.

59 S. C. Troutman, N. G. Love and B. Kerkez, Balancing Water Quality and Flows in Combined Sewer Systems Using Real-Time Control, *Environ. Sci.: Water Res. Technol.*, 2020, **6**(5), 1357–1369, DOI: 10.1039/c9ew00882a.

60 B. Kerkez, C. Gruden, M. Lewis, L. Montestruque, M. Quigley, B. Wong, A. Bedig, R. Kertesz, T. Braun, O. Cadwalader, A. Poresky and C. Pak, Smarter Stormwater Systems, *Environ. Sci. Technol.*, 2016, **50**(14), 7267–7273, DOI: 10.1021/acs.est.5b05870.

61 M. Bartos, B. Wong and B. Kerkez, Open Storm: A Complete Framework for Sensing and Control of Urban Watersheds, *Environ. Sci.: Water Res. Technol.*, 2018, **4**(3), 346–358, DOI: 10.1039/c7ew00374a.

62 L. Holtan-Hartwig, P. Dörsch and L. R. Bakken, Low Temperature Control of Soil Denitrifying Communities: Kinetics of N<sub>2</sub>O Production and Reduction, *Soil Biol. Biochem.*, 2002, **34**(11), 1797–1806, DOI: 10.1016/S0038-0717(02)00169-4.

63 C. M. Greenan, T. B. Moorman, T. B. Parkin, T. C. Kaspar and D. B. Jaynes, Denitrification in Wood Chip Bioreactors at Different Water Flows, *J. Environ. Qual.*, 2009, **38**(4), 1664–1671, DOI: 10.2134/jeq2008.0413.

64 N. L. Hoover, A. Bhandari, M. L. Soupir and T. B. Moorman, Woodchip Denitrification Bioreactors: Impact of Temperature and Hydraulic Retention Time on Nitrate Removal, *J. Environ. Qual.*, 2016, **45**, 803–812, DOI: 10.2134/jeq2015.03.0161.

65 W. T. Pluer, C. K. Morris, M. T. Walter and L. D. Geohring, Denitrifying Bioreactor Response during Storm Events, *Agric. Water Manag.*, 2019, **213**, 1109–1115, DOI: 10.1016/j.JAGWAT.2018.12.004.

66 A. M. Quick, W. J. Reeder, T. B. Farrell, D. Tonina, K. P. Feris and S. G. Benner, Controls on Nitrous Oxide Emissions from the Hyporheic Zones of Streams, *Environ. Sci. Technol.*, 2016, **50**(21), 11491–11500, DOI: 10.1021/acs.est.6b02680.

67 A. Rivas, G. Barkle, R. Stenger, B. Moorhead and J. Clague, Nitrate Removal and Secondary Effects of a Woodchip Bioreactor for the Treatment of Subsurface Drainage with Dynamic Flows under Pastoral Agriculture, *Ecol. Eng.*, 2020, **148**, 105786, DOI: 10.1016/j.ecoleng.2020.105786.

68 C. Lepine, L. Christianson, J. Davidson and S. Summerfelt, Woodchip Bioreactors as Treatment for Recirculating Aquaculture Systems' Wastewater: A Cost Assessment of Nitrogen Removal, *Aquac. Eng.*, 2018, **83**, 85–92, DOI: 10.1016/j.aquaeng.2018.09.001.

69 S. M. Cragg, G. T. Beckham, N. C. Bruce, T. D. H. Bugg, D. L. Distel, P. Dupree, A. G. Etxabe, B. S. Goodell, J. Jellison and J. E. McGeehan, *et al.*, Lignocellulose Degradation Mechanisms across the Tree of Life, *Curr. Opin. Chem. Biol.*, 2015, **29**, 108–119, DOI: 10.1016/j.cbpa.2015.10.018.

70 M. Keiluweit, P. Nico, M. E. Harmon, J. Mao, J. Pett-Ridge and M. Kleber, Long-Term Litter Decomposition Controlled by Manganese Redox Cycling, *Proc. Natl. Acad. Sci. U. S. A.*, 2015, **112**(38), E5253–E5260, DOI: 10.1073/pnas.1508945112.

71 M. E. Jones, P. S. Nico, S. Ying, T. Regier, J. Thieme and M. Keiluweit, Manganese-Driven Carbon Oxidation at Oxic-Anoxic Interfaces, *Environ. Sci. Technol.*, 2018, **52**(21), 12349–12357, DOI: 10.1021/acs.est.8b03791.